Synthesis and Properties of Polyacetylenes Containing Terphenyl Pendent Group with Different Spacers

Dan Zhou,[†] Yiwang Chen,*[,†,‡] Lie Chen,*[,‡] Weihua Zhou,[‡] and Xiaohui He[‡]

Department of Chemistry, School of Science, Nanchang University, Xuefu Road 999, Nanchang 330031, People's Republic of China, and Institute of Polymers/Institute for Advanced Study, Nanchang University, Xuefu Road 999, Nanchang 330031, People's Republic of China

Received December 1, 2008; Revised Manuscript Received January 17, 2009

ABSTRACT: Liquid-crystalline, monosubstituted acetylenes containing terphenyl pendent group with varying spacer lengths [HC≡C$(CH_2)_n$O-terphenyl-CN, **A*n*CN**, n = 1, 6] and its polymers **PA*n*CN** were synthesized. Also, the effects of the structural variation on their properties, especially their mesomorphism, UV and photoluminescence behaviors, were studied. The monomers are prepared by simple Suzuki coupling reactions. High yields and high trans-content of polyacetylenes were obtained by polymerization using $[Rh(nbd)Cl]_2$ catalyst. The polymer with long spacers (hexamethylene), that is, **PA6CN**, formed a nematic mesophase when heated and cooled, however the polymer with short spacers (methylene), that is, **PA1CN**, could not exhibit liquid crystallinity at elevated temperatures. Upon photoexcitation by keep the constant photons of excitation, **PA1CN** emits ultraviolet emission (λ_{max} ∼ 311 nm) but **PA6CN** gives a stronger emission (λ_{max}∼308 nm), indicating that the emission intensity increases with the spacer length due to orientation of main chain by alignment of mesogenic pendant. Short spacer between polyacetylene and mesogens hindered alignment of the main chain, consequently lower fluorescence emission, and loss mesophase of the polymer was induced by short spacer due to disturbance of rigid main chain.

Introduction

Liquid crystalline conjugated polymers have been extensively studied for their intriguing applications and stimulate technological innovations in the development of novel electronic and photonic devices such as liquid crystal displays (LCD), light-emitting diodes (LED), photovoltaic cells, film transistors, and plastic lasers.[1,2] The introduction of orientable mesogenic moieties onto a conjugated polymer backbone might increase the conjugation in the main chain and yield polymers with permanent coupling between electro-active properties and order. The spontaneous orientation and externally forced alignment of the mesogens enable us to control electrical and optical properties as well as their anisotropies.[3−6]

Polyacetylene is an archetypal conjugated polymer, which is well-known for its high electrical conductivity when doped with iodine of AsF_5. Compared to the instability and intractability of polyacetylene, substituted polyacetylenes show thermal stability, good solubility, excellent luminescence and photoconductivity by introducing different mesogens.[7] If the substituent is a liquid-crystalline group, the polymer is not only soluble in organic solvents, but also easily aligned by spontaneous orientation of the liquid-crystalline group. Recently, a variety of polyacetylenes containing liquid-crystalline mesogens, optical nonlinearity and light-emitting chromophores have been prepared.[8−15] The polymers have been found to show multifaceted mesophases, with their transition temperatures tunable by their molecular structures.

Conjugated polymers containing mesogenic and chromophoric units can potentially show very high carrier mobility and emit polarized light.[16] The terphenyl chromophoric core has a calamitic structure that is compatible with mesomorphic ordering and is well-known to give liquid crystals that have high birefringence.[17] Polymers containing terphenyl moieties in the main chain or side chains have been widely investigated for unique optoelectronic properties.[18] However, few terphenyl-containing conjugated polymers have been reported, although such polymers may exhibit novel optical and electronic properties. The terphenyl is not only a chromophore but also a mesogenic core.[19,20] Thus, if combining optically active terphenyl with electronically active polyacetylenes at the molecular level, the spontaneous orientation and chromophoric property of the terphenyl mesogens might likely lead to materials with novel, outstanding and interesting properties. The terphenyl mesogen groups as a pendant linked to the backbone might transfer its energy to the backbone and provide polymers with high light-emitting. For this reason, our group has attempted to design and synthesize polyacetylenes containing terphenyl pendent group with different spacer lengths. The structures and properties of the monomers and their corresponding polymers have been given special attention. We also found that the spacer length affected both the ultraviolet emission and the packing arrangement of the mesomorphic polyacetylenes.

Experimental Section

Materials. 4-Bromo-4′-hydroxybiphenyl, $[Rh(nbd)Cl]_2$, *n*-butyllithium (2.2 M in hexane, packaged under Argon in resealable), tetrakis(triphenylphosphine)palladium(0) were purchased from Alfa Aasar. 4-Bromobenzonitrile, trimethyl borate, and 1,6-dibromehexane were purchased from Aldrich, and used as received without any further purification. Tetrahydrofuran (THF) was dried over sodium, and triethylamine (Et_3N) was dried over calcium hydride and then distilled under nitrogen. Other chemicals were obtained from Shanghai Reagent Co., Ltd., and used as received.

Techniques. The nuclear magnetic resonance (NMR) spectra were collected on a Bruker ARX 400 NMR spectrometer with deuterated chloroform or THF as the solvent and with tetramethylsilane(δ=0) as the internal standard. The infrared (IR) spectra were recorded on a Shimadzu IRPrestige-21 Fourier transform infrared (FTIR) spectrophotometer by drop-casting sample solution on KBr substrates. The ultraviolet−visible (UV) spectra of the samples were recorded on a Hitachi UV-2300 spectrophotometer. Fluorescence measurement for photoluminescence (PL) of the polymers was carried out on a Shimadzu RF-5301 PC spectrof-

* Corresponding authors. Telephone: +86 791 3969562. Fax: +86 791 3969561. E-mail: (Y.C.) ywchen@ncu.edu.cn.
[†] Department of Chemistry, School of Science, Nanchang University.
[‡] Institute of Polymers/Institute for Advanced Study, Nanchang University.

10.1021/ma802686d CCC: $40.75 © 2009 American Chemical Society
Published on Web 02/11/2009

Scheme 1. Illustration of Procedures for Synthesis of PA1CN and PA6CN

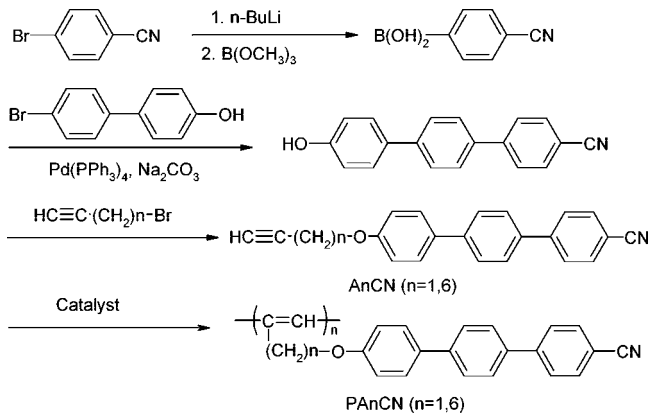

luorophotometer with a xenon lamp as the light source. The gel permeation chromatography (GPC), so-called size-exclusion chromatography (SEC) analysis, was conducted with a Breeze Waters system equipped with a Rheodyne injector, a 1515 isocratic pump and a Waters 2414 differential refractometer using polystyrenes as the standard and tetrahydrofuran (THF) as the eluent at a flow rate of 1.0 mL/min and 40 °C through a Styragel column set, Styragel HT3 and HT4 (19 mm × 300 mm, 10^3+10^4 Å) to separate molecular weight (MW) ranging from 10^2 to 10^6. Thermogravimetric analysis (TGA) was performed on a PerkinElmer TGA 7 for thermogravimetry at a heating rate of 20 °C/min under nitrogen with a sample size of 8−10 mg. Differential scanning calorimetry (DSC) was used to determine phase-transition temperatures on a Perkin-Elmer DSC 7 differential scanning calorimeter with a constant heating/cooling rate of 10 °C/min. Texture observations by polarizing optical microscopy (POM) were made with a Nikon E600POL polarizing optical microscope equipped with an Instec HS 400 heating and cooling stage. The X-ray diffraction (XRD) study of the samples was carried out on a Bruker D8 Focus X-ray diffractometer operating at 30 kV and 20 mA with a copper target (λ = 1.54 Å) and at a scanning rate of 1°/min.

Synthesis of the Monomers. The synthesis and structures of the monomers are outlined in Scheme 1. All of the reactions and manipulations were carried out under nitrogen.

4-Cyanophenylboronic Acid. 4-Bromobenzene carbonitrile 1.82 g (0.010 mol) was dissolved in 100 mL of anhydrous THF in a 250 mL three-neck flask equipped with a dropping funnel, thermometer, and nitrogen inlet−outlet. The solution was cooled to −78 °C with liquid nitrogen and ethanol. The *n*-BuLi (2.2 M in hexane) 21.10 mL was added dropwise over 0.5 h to the stirring mixture, maintaining the temperature below −78 °C. Then $B(OCH_3)_3$ (7.44 mL) in 21.00 mL of anhydrous THF was added dropwise to the stirring mixture, still maintaining the temperature below −78 °C. The reaction mixture was subsequently warmed to room temperature and stirred overnight. The dilute HCl (40.20 mL) was added dropwise, and the mixture was stirred for 1 h. The solution was extracted two times with Et_2O, washed with water, dried over $MgSO_4$ and filtered, and the solvent was evaporated to yield a white powder. The powder was dissolved in THF, precipitated in hexane, and filtered to yield a white powder, 1.36 g (yield 75.10%), which was used in the next step without further purification and characterization.

4-Hydroxy-4′-cyano-p-terphenyl. Under the protection of nitrogen, 4-bromo-4′-hydroxybiphenyl (1.64 g, 6.58 mmol), $Pd(PPh_3)_4$ (0.19 g), 1 M Na_2CO_3 (9 mL) and toluene (12 mL) were added to a 50 mL three-neck flask. 4-Cyanophenylboronic acid (1.34 g, 0.0085 mol dissolved in 9 mL 95% ethanol) was added dropwise at 80 °C. The reaction mixture was stirred at the same temperature overnight. Then the mixture was cooled to the room temperature and diluted with chloroform and water to form two phases. The organic layer was separated, dried over $MgSO_4$, and filtered, and the solvent was distilled with a rotary evaporator. The resulting product was purified by column chromatography (silica gel, dichloromethane/hexane) to yield 1.42 g (52.10%) of white powder. IR (KBr, cm^{-1}): ν 2230 (C≡N), 3351 (−OH). ^{1}H NMR (400 MHz, $CDCl_3$, ppm): δ 7.73 (d, 4H, Ar−H, J = 8.0 Hz), 7.65 (d, 4H, Ar−H, J = 6.4 Hz), 7.53 (d, 2H, Ar−H, J = 6.8 Hz), 6.93 (d, 2H, Ar−H, J = 8.4 Hz), 4.91 (s, 1H, OH).

3-[(4′-Cyano-4-terphenyl)oxy]-1-propyne. A mixture of 4-hydroxy-4′-cyano-*p*-terphenyl, 2.71 g (0.010 mol), 3-bromo-1-propyne, 1.41 g (0.012 mol), anhydrous potassium carbonate, 2.25 g (0.024 mol), and acetone, 150 mL was refluxed for 24 h under argon atmosphere. After the mixture had cooled to room temperature, the solution was filtered off, and the filtrate was evaporated. After 30 mL of ether was added into the residue quickly, the resulting white precipitate was collected by filtration. The solid was redissolved by hot acetone and reprecipitated by ether to afford 0.40 g pale yellow powder (yield 25.90%). Mp: 177−178 °C. IR (KBr, cm^{-1}): ν 2229 (C≡C, C≡N), 3031 (≡C−H), 682 (≡C−H bending). ^{1}H NMR (400 MHz, $CDCl_3$, ppm): δ 7.67 (d, 4H, Ar−H, J = 8.0 Hz), 7.60(d, 4H, Ar−H, J = 6.4 Hz), 7.48 (d, 2H, Ar−H, J = 6.8 Hz), 6.84 (d, 2H, Ar−H, J = 8.4 Hz), 4.69 (s, 2H, OCH_2), 2.49 (s, 1H, ≡CH). ^{13}C NMR (400 MHz, $CDCl_3$, ppm): δ 156.0 (aromatic carbon linked to OCH_2), 143.01 (aromatic carbon para to CN), 139.6 (terphenyl core carbons), 134.8 (aromatic carbons ortho to CN), 130.54 (aromatic carbons meta and para to OCH_2), 129.1 (aromatic carbon meta to CN), 125.8 (terphenyl core carbons), 116.3(−C≡N), 113.7 (aromatic carbon ortho to OCH_2) 109.1 (aromatic carbon linked to CN).

8-[(4′-Cyano-4-terphenyl)oxy]-1-octyne. This was obtained similarly. Yield = 72.30%; mp = 148−149 °C. IR (KBr, cm^{-1}): ν 2229 (C≡C, C≡N), 3070 (≡C−H), 637 (≡C−H bending). ^{1}H NMR (400 MHz, $CDCl_3$, ppm): δ 7.72 (d, 4H, Ar−H, J = 8.0 Hz), 7.67 (d, 4H, Ar−H, J = 6.4 Hz), 7.56 (d, 2H, Ar−H, J = 6.8 Hz), 6.98 (d, 2H, Ar−H, J = 8.4 Hz), 4.03 (s, 2H, OCH_2), 2.22 (s, 1H, ≡CH), 2.22 (m, 2H, OCH_2CH_2), 1.92 (t, 2H, CH_2C≡), 1.90 (m, 2H, CH_2CH_2C≡), 1.60 (m, 4H, $CH_2CH_2CH_2CH_2C$≡).^{13}C NMR (400 MHz, $CDCl_3$, ppm): δ 158.0 (aromatic carbon linked to OCH_2), 144.01 (aromatic carbon para to CN), 140.2 (terphenyl core carbons), 136.2 (aromatic carbons ortho to CN), 131.51 (aromatic carbons meta and para to OCH_2), 127.1 (aromatic carbon meta to CN), 125.8 (terphenyl core carbons), 116.3 (−C≡N), 113.7 (aromatic carbon ortho to OCH_2), 109.1 (aromatic carbon linked to CN).

Polymerization. All of the polymerization reactions and manipulations were carried out under nitrogen using Schlenk techniques in a vacuum line system or an inert atmosphere glovebox (Vacuum Atmospheres), except for the purification of the polymers, which was done in an open atmosphere. A typical experimental procedure for the polymerization was as follows:

Into a baked 20 mL Schlenk tube with a stopcock in the sidearm was added 0.50 g (1.62 mmol) of **A1CN**. The tube was evacuated under vacuum and then flushed with nitrogen three times through the sidearm. Freshly distilled toluene (1.8 mL) was injected into the tube to dissolve the monomer. The catalyst solution was prepared in another tube by dissolving 15.0 mg of $[Rh(nbd)Cl]_2$ in 1 mL of toluene and 4 mL of Et_3N. The two tubes were aged at 60 °C for 15 min and then the monomer solution was transferred to the catalyst solution using a hypodermic syringe. The reaction mixture was stirred at 60 °C under nitrogen for 24 h. The solution was then cooled to room temperature, diluted with 5 mL of chloroform, and added dropwise to 500 mL of acetone through a cotton filter under stirring. The precipitate was allowed to stand overnight and then filtered with a Gooch crucible. The polymer was washed with acetone and dried in a vacuum oven to a constant weight. Yellow powder: yield 81.50%.

Characterization Data. *PA1CN.* Yellow-brown powder: yield 81.50%. IR (KBr, cm^{-1}): ν 2215 (C≡N), 3038 (=CH). ^{1}H NMR (400 MHz, $CDCl_3$, ppm): δ 7.68 (d, 4H, Ar−H, J = 8.0 Hz), 7.58 (d, 4H, Ar−H, J = 6.4 Hz), 7.40 (d, 2H, Ar−H, J = 6.8 Hz), 6.83 (d, 2H, Ar−H, J = 8.4 Hz), 6.99 (s, 1H, trans, =CH), 4.26 (s, 2H, OCH_2). ^{13}C NMR (400 MHz, $CDCl_3$, ppm): δ 157.0 (aromatic carbon linked to OCH_2), 144.6 (aromatic carbon para to CN), 141.1

(terphenyl core carbons and HC═*C*), 136.3 (aromatic carbons ortho to CN), 132.1 (aromatic carbons meta and para to OCH_2), 130.4 (aromatic carbon meta to CN), 126.8 (terphenyl core carbons), 117.8 (−C≡N and *C*═*C*H), 115.2 (aromatic carbon ortho to OCH_2), 110.5 (aromatic carbon linked to CN).

PA6CN. Brown powder: yield 94.80%. IR (KBr, cm^{-1}): ν 2215 (C≡N), 3038 (═CH). ^1H NMR (400 MHz, $CDCl_3$, ppm): δ 7.98 (d, 4H, Ar−H, J = 8.0 Hz), 7.82 (d, 4H, Ar−H, J = 6.4 Hz), 7.72 (d, 2H, Ar−H, J = 6.8 Hz), 6.99 (d, 2H, Ar−H, J = 8.4 Hz), 6.38 (s, 1H, cis, ═CH), 4.01 (s, 2H, OCH_2), 1.74 (m, 2H, OCH_2CH_2), 1.49 (t, 2H, CH_2C≡), 1.21 (m, 2H, CH_2CH_2C≡), 0.82 (m, 4H, $CH_2CH_2CH_2CH_2C$≡). ^{13}C NMR (400 MHz, $CDCl_3$, ppm): δ 155.0 (aromatic carbon linked to OCH_2), 144.1 (aromatic carbon para to CN), 141.2 (terphenyl core carbons and HC═*C*), 138.2 (aromatic carbons ortho to CN), 132.4 (aromatic carbons meta and para to OCH_2), 130.3 (aromatic carbon meta to CN), 127.2 (terphenyl core carbons), 116.3 (−C≡N and *C*═*C*H), 114.5 (aromatic carbon ortho to OCH_2), 109.1 (aromatic carbon linked to CN).

Results and Discussion

Synthesis of the Monomers. The synthetic routes of the monomers are shown in Scheme 1. The acetylene monomers were synthesized through a three reaction steps: 4-cyanophenylboronic acid was prepared by of 4-bromobenzene carbonitrile in high yields (75.10%). The 4-hydroxy-4′-cyano-*p*-terphenyl was prepared through the Suzuki coupling reaction between 4-cyanophenylboronic acid and 4-bromo-4′-hydroxybiphenyl using tetrakis(triphenylphosphine)palladium(0) as the catalyst. 3-[(4′-Cyano-4-terphenyl)-oxy]-1-propyne (**A1CN**) and 8-[(4′-cyano-4-terphenyl)oxy]-1-octyne (**A6CN**) were obtained by 4-hydroxy-4′-cyano-*p*-terphenyl with propargyl bromide and 8-bromo-1-octyne via etherification. The poor yield (25.90%) in etherification of propargyl bromide and 4-hydroxy-4′-cyano-*p*-terphenyl might be due to conjugation effect of propargyl. The structures of all the intermediates and the final monomers were confirmed by FTIR, ^1H NMR, besides the final monomers and polymers were verified by ^{13}C NMR. The C≡H stretching and bending vibrations for the monomers were observed at about 3250 and 680 cm^{-1}, respectively. The monomers showed a absorption at about 2240 cm^{-1} associated with C≡C stretching vibrations, which was merged with the absorption of C≡N stretch at 2250 cm^{-1}. The structures were verified by ^1H NMR spectroscopy as well. It is noteworthy that the resonance peak at 2.51 in both of the ^1H NMR spectra of the monomers is attributable to the chemical shift of the proton in C≡H. All the intermediates and monomers were characterized by standard spectroscopic methods, from which satisfactory analysis data were obtained (see the Experimental Section for details).

Synthesis of the Polymers. Transition-metal catalysts are the most commonly used catalysts for acetylene polymerizations. Syntheses of substituted polyacetylenes containing polar groups have, however, been difficult. The polymerizations of methyl propiolate [HC≡CCO_2CH_3] and 5-cyano-1-pentyne [HC≡C-$(CH_2)_3CN$] catalyzed by $MoCl_5$−Ph_4Sn gave only oligomeric products,[21,22] meanwhile, the reaction of [HC≡$C(CH_2)_3$-CO_2−Biph−CN; biph = biphenyl] catalyzed by $MoCl_5$ in toluene, however, gave no polymeric products, maybe due to the poisoning interaction of the polar ester and cyano groups with the Mo-based catalyst systems.[23] WCl_6−Ph_4Sn is known to be effective catalysts for the polymerizations of acetylene derivatives with functional groups,[24] but it is not an effective catalyst for the polymerizations of acetylene containing cyano groups. Thus, it is even more challenging to polymerize monomer **A1CN**, **A6CN**, because they contain the polar ether and cyano units.

Rh-based compounds are the most widely used initiators for the polymerization of acetylene-based monomers with polar units.[25] We thus tried to polymerize our cyano-containing acetylene monomers **A1CN**, **A6CN** using $[Rh(nbd)Cl]_2$ as catalyst. So disappointed to us, the reaction of [HC≡C-$(CH_2)_n$O−terphenyl−CN, n = 1, 6] catalyzed by $[Rh(nbd)Cl]_2$ in toluene, however, yielded no polymeric products at room temperature, increasing the temperature to 60 °C did not help at all. Interestingly, the HC≡C−phenyl−NH−CO−$(CH_2)_{10}$-SH was successfully polymerized by $[Rh(nbd)Cl]_2$ in THF/Et_3N. However, no polymer product was obtained in the absence of Et_3N. Et_3N molecule may have coordinated with the metal center and hence protected the catalyst from the toxic effect of the mercapto group.[25] It is of interest that when the polymerization of **A*n*CN** was conducted in THF/ Et_3N, however, was encouraging: After **A*n*CN** and $[Rh(nbd)Cl]_2$ were admixed in a mixture of THF and Et_3N, the color of the reaction mixture changed from pale brown to red brown only in a few minutes. After 24 h, the reaction product was dissolved in THF, poured the dilute THF solution into acetone, and isolated the precipitate by filtration. To our delight, the yields of **A1CN and A6CN** up to 81.50%, and 94.80% were obtained, respectively. The polymerization of the acetylene monomers by the Rh complex gave polymers [**PA1CN** and **PA6CN**] with narrow polydispersity and moderate molecular weights (shown in **Table 1**) (weight-average molecular weight (M_w) =12 900 and number-average molecular weight (M_n) = 11 900 for **PA1CN**; M_w =12 000 and M_n = 9900 for **PA6CN**).

Table 1. Molecular Weights of the Polymers

polymer	M_n	M_w	MWD[a]	DP[b]
PA1CN	11900	12900	1.08	38.5
PA6CN	9900	12000	1.21	26.1

[a] MWD: molecular weight distribution. [b] DP = degree of polymerization calculated by M_n/mru (mru: molecular weight of molecular repeat unit).

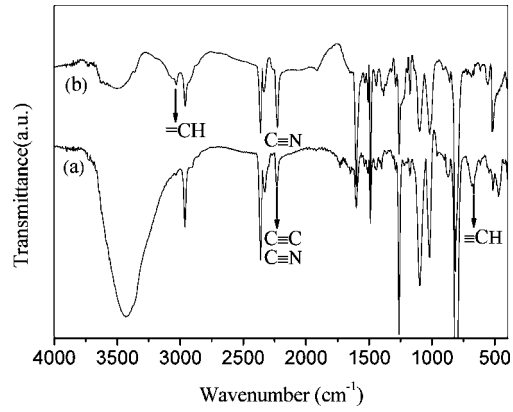

Figure 1. IR spectra of (a) **A1CN** and (b) **PA1CN**.

Structural Characterization. All the purified polymerization products gave satisfactory spectroscopic data corresponding to their expected molecular structures (see Experimental Section for details). A typical example of the IR spectra of **PA1CN** is shown in Figure 1. The spectrum of its monomer **A1CN** is also shown in the same figure for comparison. The C≡H stretching and bending vibrations for the monomer are observed at 3253 and 682 cm^{-1}, which completely disappeared in the spectra of their polymers. The absorption band of HC≡ stretching at 3253 cm^{-1} in the monomers was converted to the HC═ band at 3038 cm^{-1} in the polymeric products when the monomers were polymerized with the Rh complex catalyst. ^1H NMR analysis proves that the acetylene triple bonds have been transformed to polyene double bonds. Figure 2 shows the ^1H NMR spectra of **A1CN** and its polymer **PA1CN** in DMSO-d_6. A new broad peak appears in the olefin absorption region (δ 6.5−5.8) of polymer **PA1CN**, which was absent in the spectrum of **A1CN**. The resonance of the methylene protons next to the triple bond

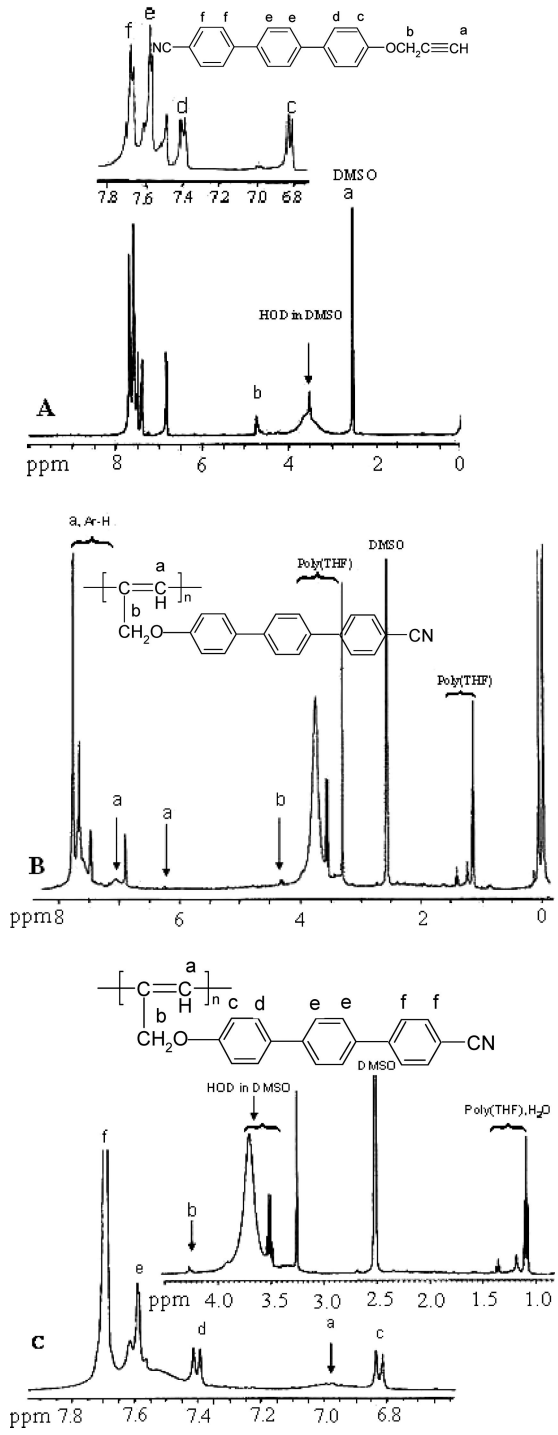

Figure 2. ^{1}H NMR spectra of (A) **A1CN** (in DMSO-d_6), and (B and C) its polymers **PA1CN** (in DMSO-d_6) prepared using $[Rh(nbd)Cl]_2$ as the catalysts.

(δ 4.68) is weakened and shift upfield (δ 4.26) after polymerization because the allenic protons (=CCH_2) are attached to a rigid polyene backbone. Masuda and Higashimura have reported that the cis olefin proton of an aliphatic poly(1-alkyne), poly(3,3-dimethyl-1-pentyne), absorbs at δ 6.05.[26] Because **PA1CN** can be viewed as a derivative of an aliphatic poly(1-alkyne) [$HC{\equiv}C(CH_2)_nOR$, n = 1, 6], where R is cyanoterphenyl, the resonance peaks of the trans proton of monosubstituted polyacetylenes are normally located in the region where aromatic protons absorb δ > 6.7).[27] It thus seems reasonable to assign the broad peak centered at δ 6.99 to the resonance by the *trans*-olefin proton and the peak centered at δ 6.26 to the resonance by the *cis*-olefin proton in the alternating double-bond backbone

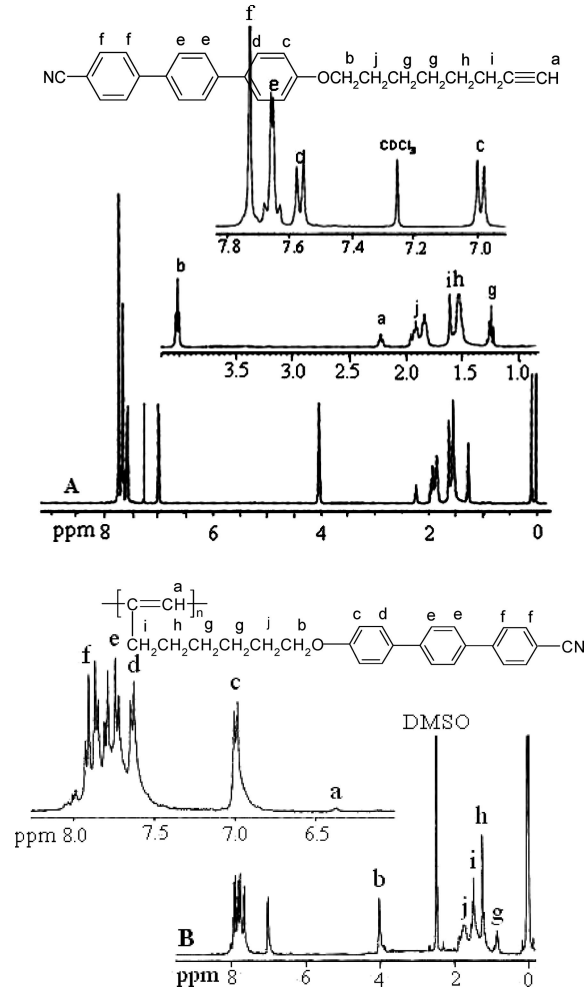

Figure 3. ^{1}H NMR spectra of (A) **A6CN** (in $CDCl_3$-d) and (B) its polymers **PA6CN** (in DMSO-d_6) prepared using $[Rh(nbd)Cl]_2$ as the catalysts.

of **PA1CN**. The cis content of the polymer can be calculated according to[11]

$$\text{cis content } (\%) = [A_{cis}/(A_{total}/13)] \times 100 \qquad (1)$$

Here A_{cis} and A_{total} are respectively the integrated peak areas of the resonance by the cis olefin proton and of the total resonance by the aromatic and olefinic protons. The cis content of **PA1CN** is calculated to be as low as 4.47% (or 95.53% trans). The polymers prepared by the Rh catalysts are normally cis-rich in stereostructure, whereas **PA*n*CN** prepared by the Rh catalysts are cis-poor or trans-rich. The high stereo effect of cyanoterphenyl mesogen forces the structure of the polymers to form trans type in order to decrease the energy of the macromolecular. The spectrum of the **PA6CN** obtained from the $[Rh(nbd)Cl]_2$ catalyst (Figure 3) was similar to that of the polymer **PA1CN.** Its cis content estimated by NMR analysis, however, was much lower 3.37% (or 96.63% trans).

Figure 4 shows the ^{13}C NMR spectrum of **A1CN** along with that of its polymer **PA1CN**. While the acetylene carbon atoms of **A1CN** absorb at δ 84.5 and 71.1, these resonances disappear in the spectrum of **PA1CN**. The resonance of the propargyl carbon of **PA1CN** at δ 58.1 also disappears owing to its transformation to the allylic structure in **PA1CN** by the acetylene polymerization. The resonances of the olefin carbon atoms of the backbone are, however, not distinguishable because of their overlapping with the peaks of the carbon atoms of the aromatic pendants. The ^{13}C NMR spectra of **A6CN** and its polymer **PA6CN** are shown in Figure 5, and have similar results.

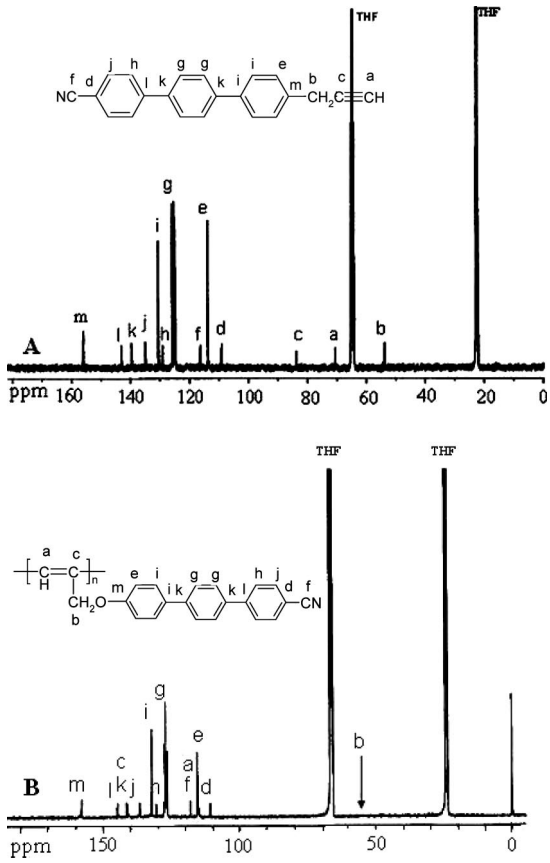

Figure 4. ^{13}C NMR spectra of **A1CN** (in THF-d_6) and its polymers **PA1CN** (in THF-d_6).

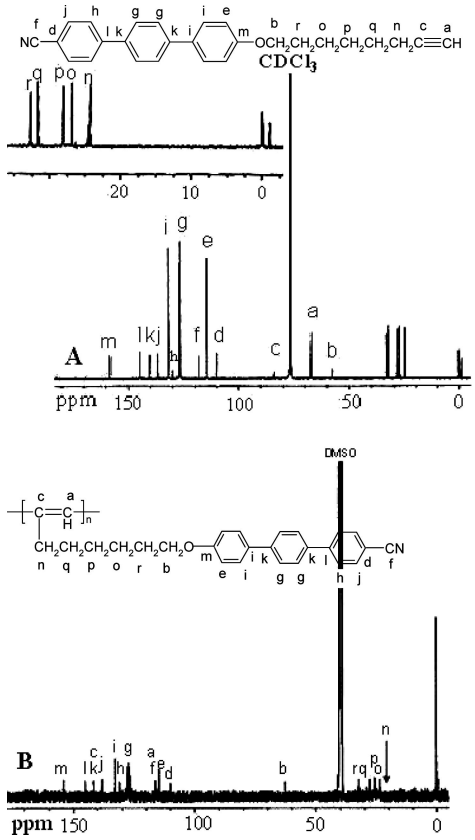

Figure 5. ^{13}C NMR spectra of **A6CN** (in $CDCl_3$-d) and its polymers **PA6CN** (in DMSO-d_6).

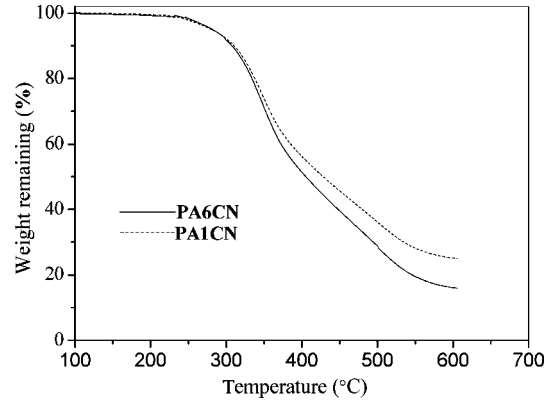

Figure 6. TGA thermograms of **PA1CN** and **PA6CN** recorded under nitrogen at a heating rate of 20 °C /min.

Thermal Stability and Liquid Crystallinity. Before investigating the mesomorphic properties of the polymers, we first examined their thermal stability. Poly(1-hexyne), a poly(1-alkyne), is so unstable that it starts to lose its weight when it is heated to a temperature as low as ~150 °C.[28] Polymers **PA1CN** and **PA6CN** are, however, thermally stable and lose almost no weight at a temperature as high as ~300 °C in the thermogravimetric analysis (Figure 6).

Figure 7 shows microphotographs of the mesomorphic textures of **A1CN**, **A6CN**, and **PA6CN** taken under a polarized optical microscope (POM). Acetylene monomers **A1CN** and **A6CN** and polymer **PA6CN** exhibited enantiotropic liquid-crystalline optical anisotropy when heated or cooled, due to the existence of terphenyl mesogen. When **A1CN** is cooled from its isotropic state, small anisotropic rhombic entities emerge from the dark background of the isotropic liquid. The fine textures grow into fanlike structures upon further cooling but the exact nature of the mesophase is difficult to identify. We repeatedly tried to grow the liquid crystals with care but stilled failed to obtain any readily identifiable characteristic textures. With the aid of X-ray diffraction (XRD) measurements, the textures are identified to be associated with a SmA_d phase (discussed later). Upon cooling the isotropic liquid of **A6CN** and **PA6CN**, birefringence textures were formed. Due to a short mesophase range of about 23 °C for **PA6CN**, a good microphotograph of textures was difficult to be taken. The polymer with one methylene unit [**PA1CN**], however, could not exhibit mesogenic phase at elevated temperatures. This suggests that the bulk and rigid side chain and the short spacer demolished the packing arrangement in the polymer.

To know more about the thermal transitions of **A*n*CN** and **PA*n*6CN**, their thermograms were measured under nitrogen on a differential scanning calorimeter (DSC) recorded during the first cooling and second heating cycles. As can be seen from Figure 8, on heating of **A1CN** at a rate of 10 °C/min^{-1}, a broad exothermic peak corresponding to recrystallization of small crystals was observed around 105.1 °C, followed by an endotherm at 138.1 °C corresponding to the k−SmA_d transition, and a strong endothermic peak appeared at 181.2 °C associated with SmA_d−i transition. In the first cooling cycle, monomer **A1CN** enters the SmA_d phase from its isotropic state at 202.3 °C. The mesophase is stable in a temperature range over 64 °C before **A1CN** finally solidifies at 138.1 °C, that is, the mesogenic phase is enantiotropic. Compared with **A1CN**, the transition profiles of **A6CN** are similar to those of **A1CN** and i−SmA and SmA−k transitions are observed at 203.7 and 129.4 °C. Polymer **PA6CN** shows two peaks at 205.9 and 182.9 °C in the first cooling cycle, the associated g−SmA and SmA−i transitions are observed at 177.8 and 201.3 °C. In sharp contrast to the polymer **PA6CN,** there is no obvious endothermic or

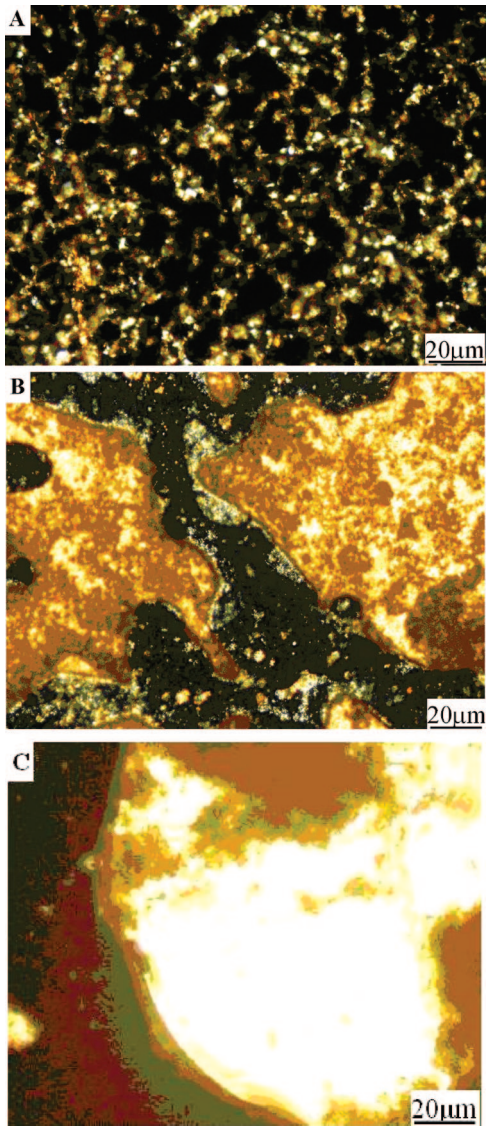

Figure 7. Mesomorphic textures observed on cooling (A) **A1CN** to 178 °C, (B) **A6CN** to 168 °C, and (C)**PA6CN** to 196 °C from their isotropic melts.

exothermic peak in the DSC curve of **PA1CN**, indicating that the polymer is not liquid crystalline.

We carried out X-ray diffraction (XRD) experiments with the aim of further verifying the mesophase assignments and gaining insights into the packing arrangements of the mesogens in the monomers and polymers. The diffractogram of **A1CN** quenched from 178 °C shows several Bragg reflections at high angles, and also displays a sharp reflection at a low-angle of $2\theta = 4.42$ Å (show in Figure 9) corresponding to a layer spacing of 19.87Å, which is in considerable excess of the molecular length of **A1CN** in its most extended conformation ($l = 15.38$ Å). The mesophase of the monomer thus may consist of such a bilayer structure as schematically shown in Figure 10, in which the mesogens arrange in an antiparallel overlapping interdigitated manner, giving a *d*/*l* ratio of 1.29, a value (about 1.4) often found in the SmA_d liquid crystalline molecules containing cyano terminal groups.[23] Because the [(cyanoterphenylyl)oxy] mesogen groups of the polymer were polarized. In order to minimize the electronic repulsive interactions, partial interdigitation of the polarized mesogens is required.[26] The XRD diffractogram of **A6CN** also displays Bragg reflections at low and middle angles. The sharp reflection at the low angle ($2\theta = 4.67°$) corresponding to a layer spacing of 19.03 Å, close to the molecular length for the repeat unit of **A6CN** at its most extended conformation (l=21.67 Å). Polymer **PA6CN**, however, shows a broad peak at $2\theta = 19.92°$ (shown in Figure 9), from which a *d*-spacing of 4.45 Å is derived from Bragg's law (**Table 2**). No reflections are observed at low angles, indicating that there exists no layer order. It is known that a nematic phase shows only a diffuse halo in a high angle region.[15] **PA1CN** shows no reflections both at low angles and high angles, indicating that there exists no liquid crystallinity, which is associated with the results of DSC and POM.

Electronic Absorption and Photoluminescence. The absorption spectra of the tetrahydrofuran (THF) solutions of the monomers and polymers are given in Figure 11. Polymers of **PA1CN** and **PA6CN** absorb strongly at 311 nm, 308 nm, respectively, which are assignable to the K bands of their terphenyl pendants, because their monomer **A1CN** and **A6CN** absorptions peak at similar wavelengths. None of the monomers shows any peaks at wavelengths longer than 359 nm, the UV spectrum of **PA6CN** well extended to beyond 450 nm. The absorption in the long-wavelength visible spectral region is thus obviously from the double-bond backbones of the polymers. The absorption, however, was quite weak. The steric crowding caused by the bulky mesogenic pendant groups might have forced the neighboring double bonds out of coplanarity, thus reducing the intensity of the absorption by the polyacetylene main chain. The UV light absorption of **PA6CN** is stronger than that of **PA1CN** while keeping a constant concentration, because the longer spacer reduces steric crowding and allows the terphenyl rings to force backbone to be more coplanar, thus resulting in the observed hyperchromic effect.

A polymer with both liquid-crystalline and light-emitting properties may find unique technological applications.[16] We thus investigated the fluorescence properties of the polymers (shown in Figure 12). Owning to the chromophoric property of the terphenyl mesogens, upon photoexcitation at 320 nm, the peak maxima of **A1CN** and **A6CN** are located at 424 and 414 nm, respectively, The PL of **PA*n*CN** are, however, observed at wavelengths longer than those of their monomers, leading to red-shift emissions with higher intensity. It suggests that the emitting center is both the mesogenic terphenyl pendant and the backbone, and energy transfer from the terphenyl pendant to the backbone favors stronger light-emitting of polyactylene. On the other hand, previous studies by Tang have revealed that light-emitting efficiencies of monosubstituted polyacetylenes are sensitive to their molecular structures.[29] The spacer lengths always affect the luminescence behaviors of the liquid crystalline poly(1-alkynes). Compared with **PA1CN,** the emission intensity of **PA6CN** is much stronger by keep the constant photons of excitation. It is in agreement with Tang's observations that a longer alkylene spacer favors stronger light emission, owing to the better segregation of the polyene backbones.[13] Meanwhile, the longer alkylene spacers may have better segregated the chromophoric pendants, which effectively hampers the excitons from traveling to the quenching sites of the polyacetylene backbone and hence enhances the chances for the confined excitons to recombine radiatively.[30]

Conclusions

In this work, the mesogenic and chromophoric cyanoterphenyl acetylene monomers and polymers with different methylene spacer lengths were designed and synthesized. The effects of the structural variations on the chemical and physical properties of the monomers and polymer were investigated. The reaction of [HC≡C$(CH_2)_n$O−terphenyl−CN, $n = 1, 6$] are successfully polymerized in high yields by $[Rh(nbd)Cl]_2$ in THF and Et_3N. Toluene is the most commonly used solvent for acetylene polymerizations but is a bad solvent for the cyanoalkyne

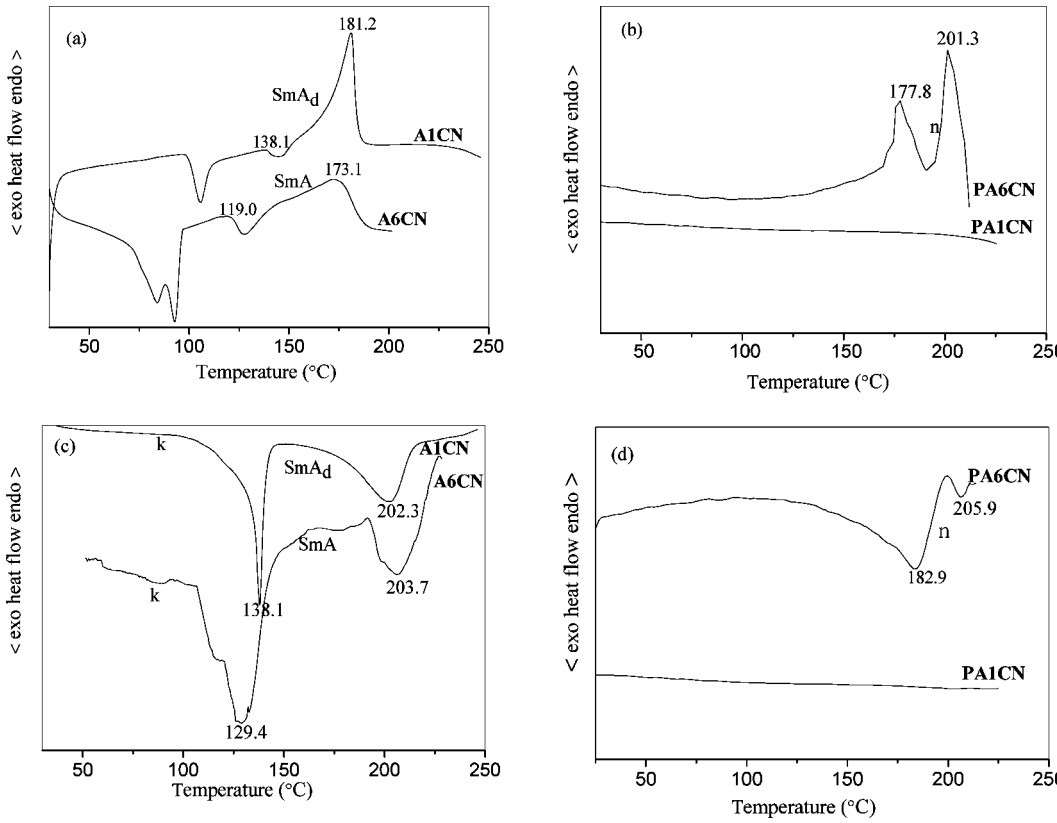

Figure 8. DSC thermograms of mesomorphic monomers and polymers recorded under nitrogen during (a, b) second heating scans and (c, d) the first cooling at a scan rate of 10 °C/min.

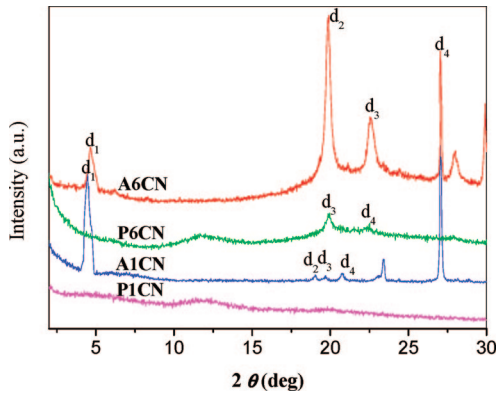

Figure 9. X-ray diffraction patterns of the mesogenic polyacetylenes and monomers quenched with liquid nitrogen from their liquid crystalline states.

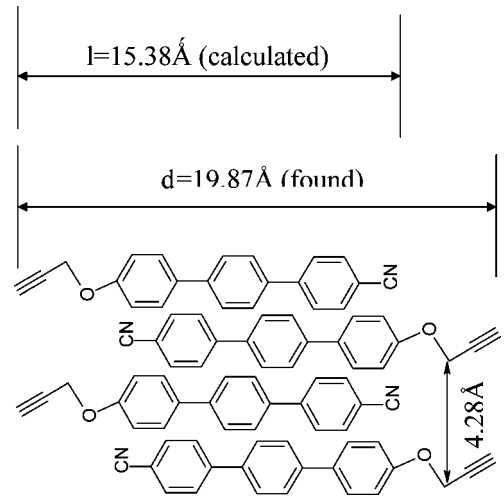

Figure 10. Proposed bilayer packing arrangement of **A1CN** within the SmA layer with the smectogens interdigitating in a head-to-tail antiparallel fashion.

polymerizations in the presence of $[Rh(nbd)Cl]_2$. When the reactions are conducted in toluene at room temperature, however, yielded no polymeric products, even though increasing the temperature to 60 °C. Thanks to the terphenyl mesogen, the monomers are all liquid crystalline and exhibit enantiotropic mesophases when heated or cooled. The spacer length exerts much influence on the liquid crystallinity, **PA6CN**, compared with the polymer with short spacer length **PA1CN**, the former possesses liquid crystallinity. However, the latter one could not exhibit liquid crystallinity at elevated temperatures. **A6CN** shows a SmA mesophase, whereas **PA6CN** shows a nematic phase due to less order than that of its monomer. The terphenyl mesogen endows the monomers and their polymers with high UV light absorption and light-emitting. Upon photoexcitation by keep the constant photons of excitation, the monomers and polymers (**A6CN** and **PA6CN**) with longer spacer lengths emit stronger light than those of monomers and polymers (**A1CN** and **PA1CN**) with shorter spacer lengths.

Table 2. X-ray Diffraction Analysis Data of A1CN, A6CN, and PA6CN

compounds	T (°C)	d_1 (Å)	d_2 (Å)	d_3 (Å)	d_4 (Å)	l (Å)[b]	ratio d_1/l	phase
A1CN	178	19.87	5.21	4.81	4.28	15.38	1.29	SmA_d
A6CN	156	19.03	5.00	4.43	3.73	21.67	0.88	SmA
PA6CN	198			4.45	3.95			n

[a] The mesophases in the liquid crystalline states at given temperatures were frozen by rapid quenching with liquid nitrogen. [b] Calculated from molecular length of monomers in their fully extended conformations.

The mesogenic and chromophoric cyanoterphenyl acetylene monomers and polymers with different methylene spacer lengths

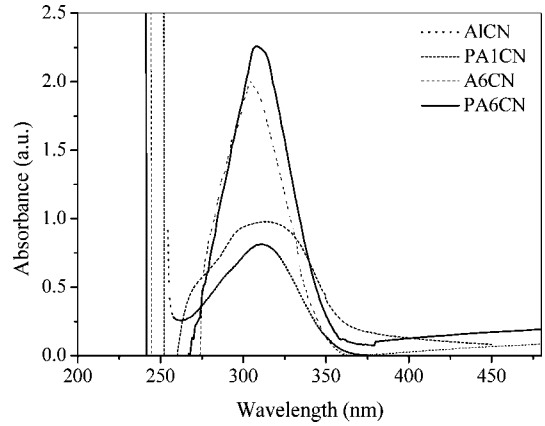

Figure 11. UV spectra of THF solutions of the monomers and the mesogenic polyacetylenes.

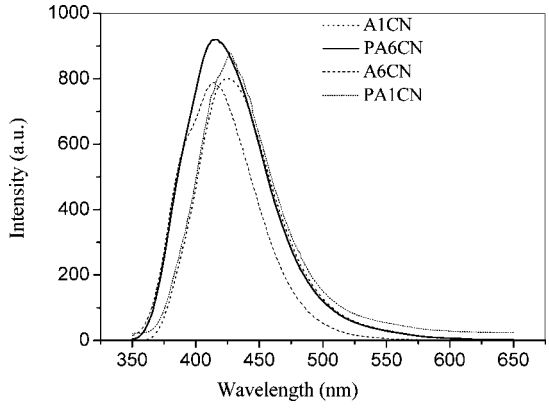

Figure 12. Photoluminescence spectra of the monomers and the mesogenic polyacetylenes in THF solutions (0.05 mM). Excitation wavelength: 320 nm.

were designed and synthesized. The presence of THF and Et_3N became necessary for polymerization of [HC≡C$(CH_2)_n$O−terphenyl−CN, $n = 1, 6$] with combination of $[Rh(nbd)Cl]_2$. The spacer length exerts much influence on the liquid crystallinity of polymers. The terphenyl mesogen endows the monomers and their polymers with high UV light absorption and light-emitting.

Acknowledgment. Financial support for this work was provided by the National Natural Science Foundation of China (50773029), the Natural Science Foundation of Jiangxi Province (520044 and 2007GZC1727), Jiangxi Provincial Department of Education, the Program for New Century Excellent Talents in University (NCET-06-0574), and the Program for Changjiang Scholars and Innovative Research Team in University (IRT0730).

References and Notes

(1) Forrest, S. R. *Nature* **2004**, *428*, 911.
(2) Heeger, A. J. *Angew. Chem., Int. Ed.* **2001**, *40*, 2591.
(3) Akagi, K.; Goto, H.; Kadokura, Y.; Shirakawa, H.; Oh, S.-Y.; Araya, K. *Synth. Met.* **1995**, *69*, 13.
(4) Akagi, K.; Goto, H.; Shirakawa, H.; Nishizawa, T.; Masuda, K. *Synth. Met.* **1995**, *69*, 33.
(5) Dai, X.-M.; Goto, H.; Akagi, K. *Mol. Cryst. Liq. Cryst.* **2001**, *365*, 347.
(6) Akagi, K.; Goto, H.; Shirakawa, H. *Synth. Met.* **1997**, *84*, 307.
(7) Law, C. C. W.; Lam, J. W. Y.; Qin, A.; Dong, Y.; Kwok, H. S.; Tang, B. Z. *Polymer* **2006**, *47*, 6642.
(8) Chen, L.; Chen, Y. W.; Zha, D. J.; Yang, Y. *J. Polym. Sci., Part A: Polym. Chem.* **2006**, *44*, 2499.
(9) Hua, J. L.; Lam, J. W. Y.; Yu, X. M.; Wu, L. J.; Kwok, H. S.; Wong, K. S.; Tang, B. Z. *J. Polym. Sci., Part A: Polym. Chem* **2008**, *46*, 2025.
(10) Wang, R.; Wang, W. Z.; Yang, G. Z.; Liu, T. X.; Yu, J. S.; Jiang, Y. D. *J. Polym. Sci., Part A: Polym. Chem.* **2008**, *46*, 790.
(11) Lam, J. W. Y.; Dong, Y. P.; Cheuk, K. K. L.; Luo, J. D.; Xie, Z. L.; Kwok, H. S.; Mo, Z. S.; Tang, B. Z. *Macromolecules* **2002**, *35*, 1229.
(12) Sanda, F.; Nakai, T.; Kobayashi, N.; Masuda, T. *Macromolecules* **2004**, *37*, 2703.
(13) Lam, J. W. Y.; Qin, A. J.; Dong, Y. P.; Lai, L. M.; Haussler, M.; Dong, Y. Q.; Tang, B. Z. *J. Phys. Chem. B* **2006**, *110*, 21613.
(14) Xing, C. M.; Lam, J. W. Y.; Zhao, K. Q.; Tang, B. Z. J. *Polym. Sci.: Part A: Polym. Chem.* **2008**, *46*, 2960.
(15) Dong, Y. P.; Lam, J. W. Y.; Peng, H.; Cheuk, K. K. L.; Kwok, H. S.; Tang, B. Z. *Macromolecules* **2004**, *37*, 6408.
(16) O'Neill, M.; Kelly, S. M. *Adv. Mater.* **2003**, *15*, 1135.
(17) Goulding, M.; Greenfield, S. M.; Parri, O.; Coates, D. *Mol. Cryst. Liq. Cryst.* **1995**, *265*, 27.
(18) Zhi, J. G.; Zhu, Z. G.; Liu, A. H.; Cui, J. X.; Wan, X. H.; Zhou, Q. F. *Macromolecules* **2008**, *41*, 1594.
(19) Oriol, L.; Piñol, M.; Serrano, J. L.; Martínez, C.; Alcalá, R.; Cases, R.; Sánchez, C. *Polymer* **2001**, *42*, 2737.
(20) Gray, G. W.; Harrison, K. J.; Nash, J. A. J. *Chem. Soc. Chem. Commun.* **1974**, *11*, 431.
(21) Masuda, T.; Kawai, M.; Higashimura, T. *Polymer* **1982**, *23*, 744.
(22) Carlini, C.; Chien, J. C. W. *J. Polym. Sci.: Polym. Chem. Ed.* **1984**, *22*, 2749.
(23) Tang, B. Z.; Kong, X. X.; Wan, X. H.; Peng, H.; Lam, W. Y. *Macromolecules* **1998**, *31*, 2419.
(24) Percec, V.; Yourd, R. *Macromolecules* **1988**, *21*, 3379.
(25) Xu, H. P.; Jin, J. K.; Mao, Y.; Sun, J. Z.; Yang, F.; Yuan, W. Z.; Dong, Y. Q.; Wang, M.; Tang, B. Z. *Macromolecules* **2008**, *41*, 3874.
(26) Okano, Y.; Masuda, T.; Higashimura, T. *J. Polym. Sci.: Polym. Chem. Ed.* **1985**, *23*, 2527.
(27) Tang, B. Z.; Kong, X. X.; Wan, X. H. *Macromolecules* **1997**, *30*, 5620.
(28) Lam, J. W. Y.; Dong, Y. P.; Law, C. C. W.; Dong, Y. Q.; Cheuk, K. K. L.; Lai, L. M.; Li, Z.; Sun, J. Z.; Chen, H. Z.; Zheng, Q.; Kwok, H. S.; Wang, M.; Feng, X. D.; Shen, J. C.; Tang, B. Z. *Macromolecules* **2005**, *38*, 3290.
(29) Huang, Y. M.; Lam, J. W. Y.; Cheuk, K. K. L.; Ge, W. K.; Tang, B. Z. *Macromolecules* **1999**, *32*, 5976.
(30) Frolov, S. V.; Fujii, A.; Chinn, D.; Hirohata, M.; Hidayat, R.; Taraguchi, M.; Masuda, T.; Yoshino, K.; Vardeny, Z. V. *Adv. Mater.* **1998**, *10*, 869.

MA802686D